Characterization and Multiscale Modeling of the Magneto-Elastic Behavior of Galfenol

Mathieu Domenjoud[1,2], Alexis Pecheux[1,2,3], and Laurent Daniel[1,2]

[1]Université Paris-Saclay, CentraleSupélec, CNRS, Laboratoire de Génie Électrique et Électronique de Paris, 91192 Gif-sur-Yvette, France
[2]Sorbonne Université, CNRS, Laboratoire de Génie Électrique et Électronique de Paris, 75252 Paris, France
[3]Université Paris-Saclay, ENS Paris-Saclay, CNRS, SATIE, 91190 Gif-sur-Yvette, France

The properties of giant magnetostrictive materials (GMMs) in actuation, sensing, or energy harvesting applications are very sensitive to pre-stress levels. This work presents the experimental characterization of the magneto-mechanical behavior of Galfenol under static compressive and tensile stress. The results show the high sensitivity of both magnetization and strain to the stress level. A multiscale modeling tool is then used to model the measured magnetic and magnetostrictive responses. The results demonstrate the ability of the proposed multiscale approach to capture the magneto-elastic effects with a very limited number of material parameters.

***Index Terms*— ⟨100⟩ fiber, crystallographic texture, hysteretic and anhysteretic behavior, magnetostriction strain, multiscale model, uniaxial tension and compression, Villari effect.**

I. Introduction

GIANT magnetostrictive materials (GMMs), such as Terfenol-D or Galfenol, can be integrated into actuation, sensing, or energy harvesting applications [1], [2], [3]. The design of these systems based on these two materials is optimized based on a good knowledge of the material properties. In operation or during the processing stages, GMM are subjected to mechanical stress that can modify their magneto-mechanical behavior [4], [5]. Therefore, it is important to characterize and model their response under magneto-mechanical loading.

Terfenol-D is well known for its high magnetostriction level (up to 1600×10^{-6}) at a high magnetic field (100 kA/m) and for being brittle. Galfenol reaches a lower maximum magnetostriction level (up to 400×10^{-6}), but keeps moderate magnetostriction (up to 270×10^{-6}) at relatively low magnetic fields (20 kA/m), exhibits low magnetic hysteresis and a higher (20 times) tensile strength. Furthermore, Galfenol can be conventionally machined [6].

While Terfenol-D magneto-mechanical behavior is very well documented in the literature, only a few works have investigated the experimental characterization [5], [7], [8], [9], [10] and the modeling [3], [9], [10], [11] aspects of the magneto-mechanical behavior of Galfenol polycrystal. These studies are restricted to hysteretic characterizations without studying the transverse magnetostriction strain. We report here the results of the magneto-mechanical characterization of a Galfenol polycrystalline sample under tensile and compressive stress. The effects of uniaxial stress on hysteretic and anhysteretic magnetic and magnetostrictive behavior are analyzed.

Manuscript received 27 March 2023; revised 23 May 2023; accepted 24 May 2023. Date of publication 29 May 2023; date of current version 24 October 2023. Corresponding author: M. Domenjoud (e-mail: mathieu.domenjoud@centralesupelec.fr).

Color versions of one or more figures in this article are available at https://doi.org/10.1109/TMAG.2023.3280925.

Digital Object Identifier 10.1109/TMAG.2023.3280925

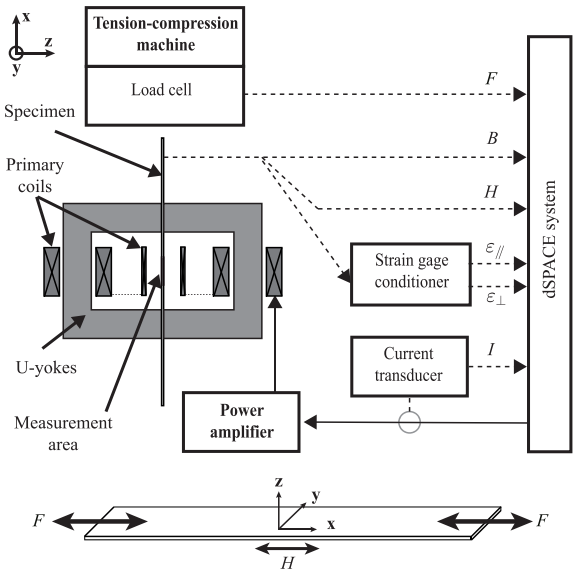

Fig. 1. Magneto-mechanical characterization rig, measurement setup and definition of the sample coordinate system (full details and real image of the setup can be found in [13]).

A multiscale modeling tool is then implemented, and its results are compared to the experimental measurements.

II. Magneto-Mechanical Characterization Setup

An experimental setup dedicated to the characterization of magneto-mechanical behavior under constant uniaxial stress [12] has been used for this study. A magnetic circuit is inserted into an electromechanical tension-compression machine (Fig. 1). The magnetic circuit, constituted of two U-shaped iron silicon alloy (FeSi), ensures the closure of the magnetic field generated by three primary coils (500 turns for external coils and 32 turns for internal coil of 16 AWG wire), powered by a current amplifier (Kepco 72–14 MG).

The current I is measured and controlled thanks to a current transducer (LA 125-P) and a control system (dSPACE). A tension-compression machine (Zwick/Roell Z030) and a load cell (Xforce P) are used to apply and control the force F along direction **x**. The stress-level σ is calculated by dividing the force applied by the initial cross section of the material (tensile stress is positive). Classical jaws grip an amagnetic material (10 mm width) glued on each face of the extremities of the sample (to avoid leakage field in the machine). The magnetic field H and the variation of magnetic induction B are measured using a Hall probe (AS-LTM) and calculated through the integration of the induced voltage of a B-coil wound around the sample (72 turns), respectively. The longitudinal (xx) and transverse (yy) strain (noted $\varepsilon_{//}$ and $\varepsilon_{\perp}$, respectively) are obtained through rosette strain gages glued on its surface and connected to a strain gauge conditioner–amplifier (Vishay 2120B). The reference state for the evaluation of B, $\varepsilon_{//}$ and $\varepsilon_{\perp}$ is the demagnetized state under stress level [13].

All measurements are performed on textured polycrystalline Galfenol (nominal composition $Fe_{81.6}Ga_{18.4}$) from TdVib LLC, USA, with preferential orientation $\langle 001 \rangle$ along the length of the sample. The sample dimensions are 250 mm (**x**) × 20 mm (**y**) × 2 mm (**z**).

III. Magneto-Elastic Measurements

Hysteretic and anhysteretic measurements (see [12], [14] for details) have been performed for 21 uniaxial stress conditions: 1) stress-free; 2) ten compressive stress levels; and 3) ten tensile stress levels from −70 to +45 MPa. A triangle current waveform (0.1 Hz under tension and 0.05 Hz under compression) has been applied to ensure accurate stress force control of the tension-compression machine. Under compression stress, the three primary coils are used to reach a maximum magnetic field close to 55 kA/m. The two external coils are disconnected under tension stress to ensure more accurate current control at lower field (up to 8 kA/m). Dynamic stress variations induced by magnetic excitation remain below 1 MPa (maximum value when magnetostriction variation is not perfectly controlled). All data are recorded at a sampling frequency of 1 kHz. Error bars on each anhysteretic figure are calculated according to the error estimation procedure described in [13]. Figs. 2 and 3 show the hysteretic (two superimposed loops) magnetic and magnetostrictive behavior of Galfenol under tensile and compressive stress levels. For better legibility, due to the difference in the magnetic field scale, tension and compression results are presented separately.

As commonly observed, the magnetic behavior of Galfenol is very sensitive to stress levels. The shape and level of magnetization and longitudinal magnetostriction are consistent with results found in the literature [3], [5], [6], [7], [8], [10]. The decrease (resp. increase) of magnetic induction with applied compression (resp. tension), for a given magnetic field, is very significant and nonlinear. Such magneto-elastic effect is expected for materials with positive longitudinal magnetostriction [15]. The width of the hysteresis loops is very thin, confirming that dissipative effects are second order compared to reversible magneto-elastic effects. Under compressive stress, a dramatic change of permeability at low and moderate magnetic fields is observed, with an inflection of the magnetization curves (as a result of 90° domain wall motion contributing in higher proportion under compressive stress).

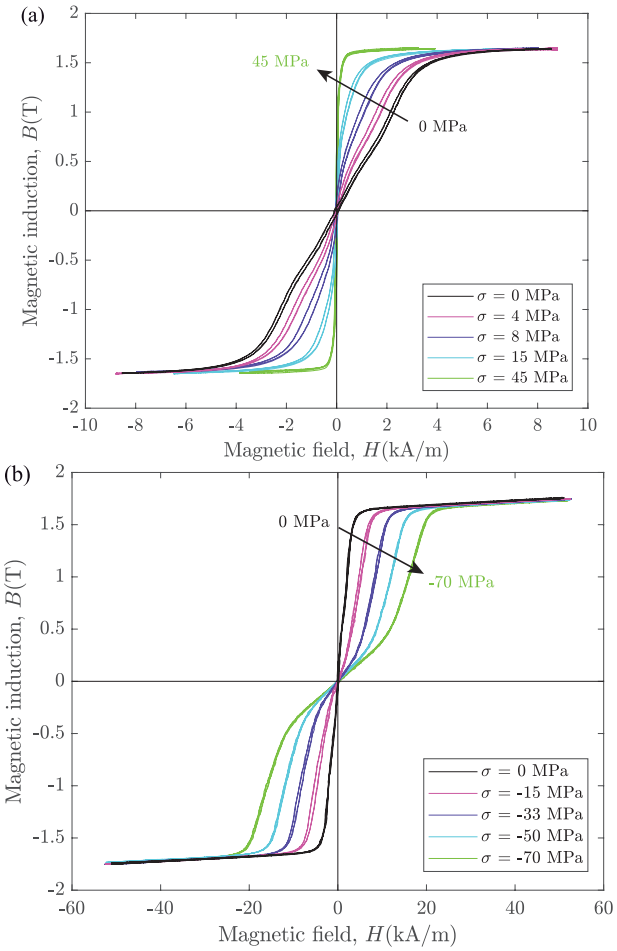

Fig. 2. Experimental results for the hysteretic magnetic behavior of Galfenol under different levels of uniaxial (a) tensile and (b) compressive stress (σ).

Magnetostrictive behavior is also very affected by stress. As a result of the ΔE effect [16], the maximum magnetostriction level decreases to 0 as the tension stress increases, and increases up to a maximum value (close to 260×10^{-6}) as the compressive compression stress increases. The effect of stress on magnetostriction is not monotonic: the application of a given stress can increase or decrease the magnetostriction level, depending on the magnetic field level. As expected, when applying a magnetic field, $\varepsilon_{\perp}$ follows the same trend as $\varepsilon_{//}$ with opposite sign. It can be noticed that the amplitude of the transverse strain is not half the amplitude of the longitudinal strain, as would be expected for an isotropic material (under isochoric assumption). The ratio $r = \varepsilon_{\perp}/\varepsilon_{//}$ evaluated close to saturation is comprised between −0.25 and −0.2, whatever the level of stress.

Anhysteretic measurements have also been conducted for the same mechanical loading conditions. Measurement results (all perfectly included inside the hysteresis loops) are presented and discussed through the comparison with modeling results in Section V.

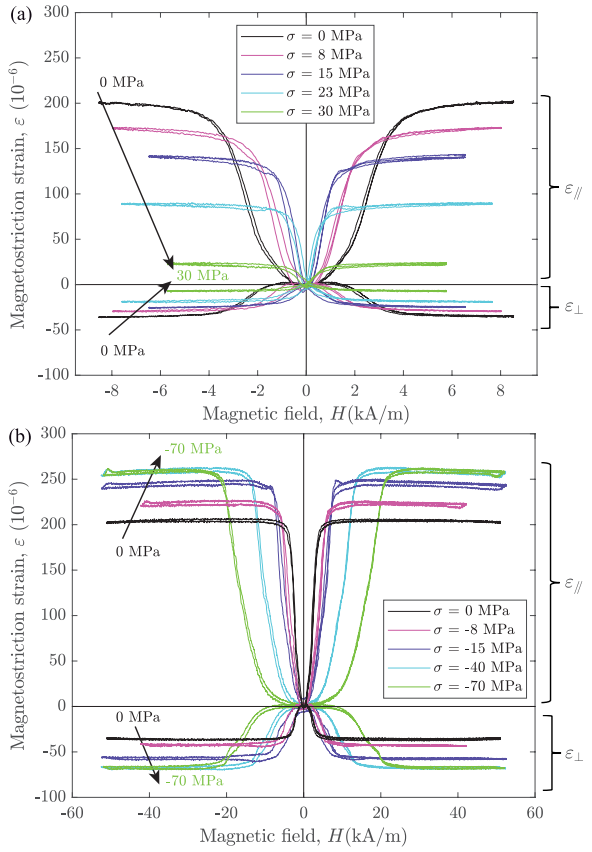

Fig. 3. Experimental results for the hysteretic longitudinal ($\varepsilon_{//}$) and transverse ($\varepsilon_{\perp}$) magnetostrictive behavior of Galfenol under different levels of uniaxial (a) tensile and (b) compressive stress (σ).

IV. Multiscale Model

A multiscale approach is used for the description of the magneto-elastic behavior [17], [18]. It is based on an energy description of the equilibrium at the domain scale. The general principle is briefly recalled hereafter.

A domain α is defined as a region where the magnetization $\mathbf{m}_\alpha$ and magnetostriction strain $\boldsymbol{\varepsilon}^\mu_\alpha$ are assumed to be uniform. Their definition (assuming a cubic symmetry for $\boldsymbol{\varepsilon}^\mu_\alpha$) is given by the following equation:

$$\mathbf{m}_\alpha = M_s\,\boldsymbol{\alpha} = M_s\,{}^t[\alpha_1 \quad \alpha_2 \quad \alpha_3] \tag{1}$$

$$\boldsymbol{\varepsilon}^\mu_\alpha = \frac{3}{2}\begin{pmatrix} \lambda_{100}\left(\alpha_1^2-\frac{1}{3}\right) & \lambda_{111}\alpha_1\alpha_2 & \lambda_{111}\alpha_1\alpha_3 \\ \lambda_{111}\alpha_1\alpha_2 & \lambda_{100}\left(\alpha_2^2-\frac{1}{3}\right) & \lambda_{111}\alpha_2\alpha_3 \\ \lambda_{111}\alpha_1\alpha_3 & \lambda_{111}\alpha_2\alpha_3 & \lambda_{100}\left(\alpha_3^2-\frac{1}{3}\right) \end{pmatrix} \tag{2}$$

where M_s is the saturation magnetization of the material, and $(\alpha_1, \alpha_2, \alpha_3)$ are the direction cosines of the magnetization in the domain α. λ_{100} and λ_{111} are the saturation magnetostriction constants of the crystal along the directions $\langle 100\rangle$ and $\langle 111\rangle$, respectively.

The free energy $\mathcal{W}_\alpha$ of a magnetic domain α is decomposed as the sum of four terms as follows:

$$\mathcal{W}_\alpha = \mathcal{W}^{\text{mag}}_\alpha + \mathcal{W}^{\text{an}}_\alpha + \mathcal{W}^{\sigma}_\alpha + \mathcal{W}^{\text{conf}}_\alpha \tag{3}$$

$\mathcal{W}^{\text{mag}}_\alpha$ is the magnetostatic energy as follows. It tends to favor domains with magnetization $\mathbf{m}_\alpha$ aligned with the applied magnetic field $\mathbf{H}$. μ_0 is the vacuum permeability

$$\mathcal{W}^{\text{mag}}_\alpha = -\mu_0\,\mathbf{H}.\mathbf{m}_\alpha \tag{4}$$

$\mathcal{W}^{\text{an}}_\alpha$ is the magnetocrystalline anisotropy energy. It tends to favor magnetization $\mathbf{m}_\alpha$ oriented along the easy axes. It is given by the following equation in the case of a cubic symmetry. K_1 and K_2 denote the magnetocrystalline anisotropy constants of the material:

$$\mathcal{W}^{\text{an}}_\alpha = K_1\left(\alpha_1^2\alpha_2^2+\alpha_2^2\alpha_3^2+\alpha_3^2\alpha_1^2\right) + K_2\left(\alpha_1^2\alpha_2^2\alpha_3^2\right) \tag{5}$$

$\mathcal{W}^{\sigma}_\alpha$ is the magneto-elastic energy, incorporating the effect of stress on the domain equilibrium. It is given by the following equation where $\boldsymbol{\sigma}$ is the second-order stress tensor:

$$\mathcal{W}^{\sigma}_\alpha = -\boldsymbol{\sigma} : \boldsymbol{\varepsilon}^\mu_\alpha \tag{6}$$

$\mathcal{W}^{\text{conf}}_\alpha$ is a complementary term that can be introduced to consider the possible bias in the initial domain configuration, created for instance by residual stresses or shape anisotropy [19]. This configuration term (7) was chosen here as the result of the effect of a (fictitious) uniaxial prestress σ_0. The prestress was set as $\sigma_0\,\mathbf{z}\otimes\mathbf{z}$, so that the configuration energy is given by the following equation. It can be noted that, given the crystallographic texture of the material (see below), the ratio r would be -0.5 in the absence of the configuration term

$$\mathcal{W}^{\text{conf}}_\alpha = \sigma_0\,{}^t\mathbf{z}\cdot\boldsymbol{\varepsilon}^\mu_\alpha\cdot\mathbf{z}. \tag{7}$$

For a given single crystal, the free energy $\mathcal{W}_\alpha$ can be evaluated in any direction $\boldsymbol{\alpha}$. In practice, the icosphere discretization of a unit sphere can be used [17]. Once the free energy $\mathcal{W}_\alpha$ is known for all domain families α, the volume fractions f_α of domain families α are introduced as internal variables. These internal variables can be calculated according to an explicit Boltzmann-type relation as follows:

$$f_\alpha = \frac{\exp(-A_s\,\mathcal{W}_\alpha)}{\sum_\alpha \exp(-A_s\,\mathcal{W}_\alpha)} \tag{8}$$

where A_s is a material parameter, proportional to the initial slope χ^o of the unstressed anhysteretic magnetization curve $A_s = 3\chi^o/\mu_0 M_s^2$ [20].

From the magnetization (1), magnetostriction strain (2) and volume fraction (8) of each domain family α, the magnetization and magnetostriction strain at the single crystal scale are obtained through a volume average over the single crystal. Since the material is polycrystalline, the operation was repeated for different grain orientations, representative for the crystallographic texture of the material. In the case of the tested material showing a strong fiber texture [10], we used a perfect $\langle 001\rangle$ fiber composed of 72 regularly distributed crystallographic orientations. The corresponding representation of the crystallographic texture used in the modeling is given in Fig. 4.

The magnetization $\mathbf{M}$ and magnetostriction strain $\boldsymbol{\varepsilon}^\mu$ of the material were finally obtained by a volume average over all the grain orientations as follows:

$$\mathbf{M} = \langle \mathbf{m}_\alpha \rangle \quad \text{and} \quad \boldsymbol{\varepsilon}^\mu = \left\langle \boldsymbol{\varepsilon}^\mu_\alpha \right\rangle. \tag{9}$$

The material parameters for the single crystal (M_s, λ_{100}, λ_{111}, K_1, K_2) were taken from the literature. Only two

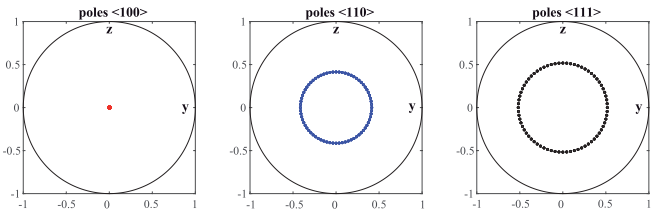

Fig. 4. ⟨100⟩, ⟨110⟩, and ⟨111⟩ pole figures for the simulated perfect fiber texture (72 orientations).

TABLE I
MODELING PARAMETERS

Parameter	M_s	$(\lambda_{100}, \lambda_{111})$	(K_1, K_2)	A_s	σ_0
Value	$13.8\,10^5$	(150, -15)	$(1, 0)\,10^4$	$2\,10^{-3}$	15
Unit	A/m	ppm	J/m^3	m^3/J	MPa
Source	[21]	[21]	[4]	Meas.	Meas.

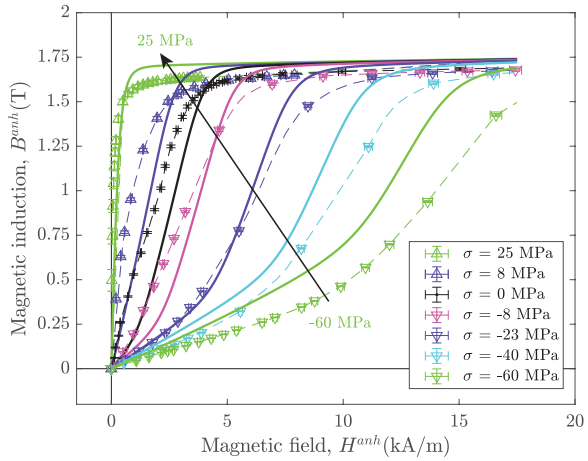

Fig. 5. Experimental (markers with error bars) and modeling (solid lines) results for the anhysteretic magnetic behavior of Galfenol under different levels of uniaxial tensile and compressive stress (σ). The dashed lines are guides for the eye.

material parameters must be extracted from experimental measurements. A_s can be identified from the initial slope of the stress-free anhysteretic magnetization curve and the configuration stress is chosen so as to approximately fit the saturation longitudinal magnetostriction strain for the unstressed material, while maintaining consistent level for the ratio r. All the material parameters used are summarized in Table I.

V. COMPARISON BETWEEN ANHYSTERETIC EXPERIMENTAL AND MODELING RESULTS

Fig. 5 shows the modeling and experimental results for the magnetization curves of Galfenol under tensile and compressive stress. The main trends are correctly described by the model. The effect of positive and negative stresses is captured at low field but presents more discrepancy at higher magnetic fields.

Fig. 6 shows the modeling and experimental results for the magnetostriction curve under tensile and compressive stress. For a better legibility, results for tension (top) and compression (bottom) are presented in different graphs. For all investigated

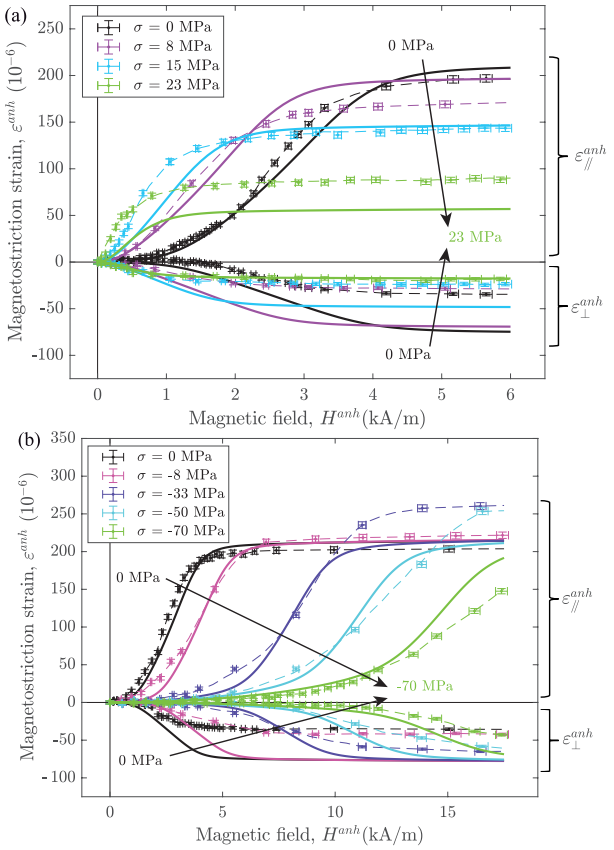

Fig. 6. Experimental (markers with error bars) and modeling (solid lines) results for the anhysteretic longitudinal ($\varepsilon^{\text{anh}}_{//}$) and transverse ($\varepsilon^{\text{anh}}_{\perp}$) magnetostrictive behavior of Galfenol under different levels of uniaxial (a) tensile and (b) compressive stress (σ). The dashed lines are guides for the eye.

stress levels, the modeling results correctly reproduce the general trend of the experimental magnetostrictive measurements, showing that the multiscale model incorporates the main mechanisms for the macroscopic behavior. However, the saturation level for the longitudinal magnetostriction strain is underestimated. Similarly, the transverse magnetostriction strain is overestimated (so that the ratio r tends to be overestimated). This might be attributed to an approximation in the single crystal material parameters, which values were taken from the literature, for materials not necessarily strictly identical in terms of composition or fabrication process. Such discrepancy can also be associated with an inaccurate description of anisotropy (choice made for the crystallographic texture) or more likely with the initial configuration energy term (choice made for the form of the configuration energy). A better choice, possibly with more than a single material parameter σ_0, could be made to account for the observation that initial domain configuration is not transverse isotropic, as demonstrated by the value of the ratio r, different from 0.5.

Fig. 7 shows the comparison between modeling and experimental results for the anhysteretic magnetic permeability (μ_{anh}, secant definition) and magnetostriction strain, obtained at different levels of magnetic field, as a function of the applied uniaxial stress. As described in Section III, the experimental results are only available in compression when applying

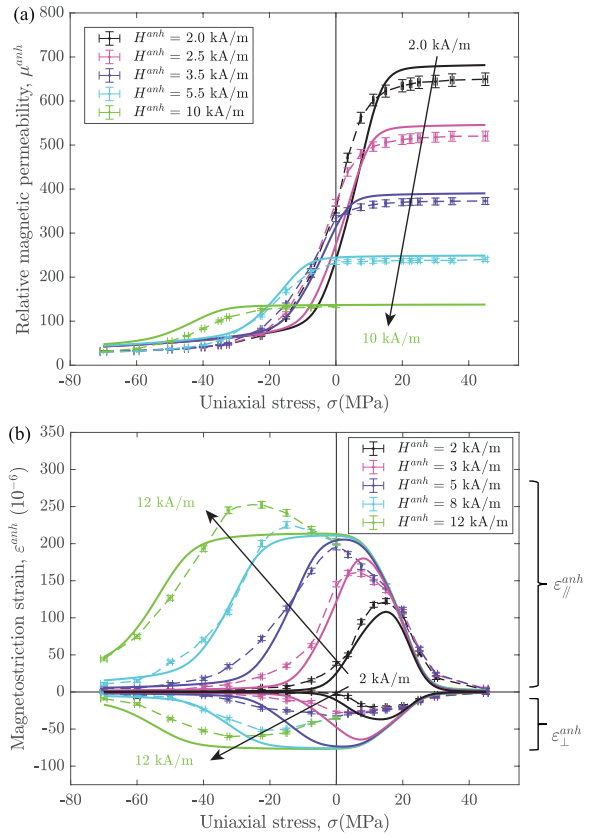

Fig. 7. (a) Experimental (markers with error bars) and modeling (solid lines) results for the anhysteretic magnetic permeability. (b) Longitudinal ($\varepsilon^{\text{anh}}_{//}$) and transverse ($\varepsilon^{\text{anh}}_{\perp}$) magnetostrictive behavior of Galfenol for different values of anhysteretic magnetic field (H^{anh}) as a function of uniaxial stress. The dashed lines are guides for the eye.

magnetic field beyond 8 kA/m. These two figures confirm the ability of the multiscale model to predict the main features of the magneto-mechanical behavior of Galfenol. As previously observed, the results are less accurate for the description of transverse magnetostrictive behavior.

VI. Conclusion

This work reports an experimental and modeling investigation on the magneto-elastic behavior of a Galfenol polycrystal subjected to tensile and compressive stress. The high sensitivity of the magnetic and magnetostrictive behavior to stress is highlighted. The hysteresis of the behavior is shown to be very weak so that an anhysteretic modeling approach appears appropriate. A magneto-elastic modeling tool, including a description of the fiber crystallographic texture of the material, is implemented. Despite a very limited number of material parameters, the proposed modeling approach is shown to satisfactorily describe the main features of the magnetic and magnetostrictive behavior of Galfenol. Higher discrepancies are found regarding the transverse magnetostriction strain, which is attributed to an imperfect description of the crystallographic texture or of the initial domain configuration of the material. It is reminded that the proposed modeling approach is based on the use of seven material parameters only: five were taken from published literature, and the two others were extracted from stress-free magneto-elastic characterization.

References

[1] J. L. Butler, *Application Manual for the Design of ETREMA Terfenol-D Magnetostrictive Transducers*. Ames, IA, USA: ETREMA Products, 1988.

[2] Z. Deng and M. J. Dapino, "Review of magnetostrictive materials for structural vibration control," *Smart Mater. Struct.*, vol. 27, no. 11, Nov. 2018, Art. no. 113001.

[3] U. Ahmed, U. Aydin, L. Daniel, and P. Rasilo, "3-D magneto-mechanical finite element analysis of galfenol-based energy harvester using an equivalent stress model," *IEEE Trans. Magn.*, vol. 57, no. 2, pp. 1–5, Feb. 2021.

[4] A. E. Clark, J. B. Restorff, M. Wun-Fogle, T. A. Lograsso, and D. L. Schlagel, "Magnetostrictive properties of body-centered cubic Fe-Ga and Fe-Ga-Al alloys," *IEEE Trans. Magn.*, vol. 36, no. 5, pp. 3238–3240, Sep. 2000.

[5] A. Mahadevan, P. G. Evans, and M. J. Dapino, "Dependence of magnetic susceptibility on stress in textured polycrystalline $Fe_{81.6}Ga_{18.4}$ and $Fe_{79.1}Ga_{20.9}$ galfenol alloys," *Appl. Phys. Lett.*, vol. 96, no. 1, Jan. 2010, Art. no. 012502.

[6] E. Summers, "Galfenol—A new class of magnetostrictive materials (galfenol public release v.7)," ETREMA Products, Ames, IA, USA, Tech. Rep., 2017. [Online]. Available: http://www.tdvib.com/wp-content/uploads/2015/07/Galfenol-Public-Release_v7edit1.pdf

[7] M. Wun-Fogle, J. B. Restorff, and A. E. Clark, "Magnetomechanical coupling in stress-annealed Fe–Ga (galfenol) alloys," *IEEE Trans. Magn.*, vol. 42, no. 10, pp. 3120–3122, Oct. 2006.

[8] J. B. Restorff and M. Wun-Fogle, "Temperature dependence of the magnetostriction of stress annealed galfenol measured under tension," *J. Appl. Phys.*, vol. 107, no. 9, May 2010, Art. no. 09A913.

[9] Z. Deng, J. J. Scheidler, V. M. Asnani, and M. J. Dapino, "Quasi-static major and minor strain-stress loops in textured polycrystalline $Fe_{81.6}Ga_{18.4}$ galfenol," *J. Appl. Phys.*, vol. 120, no. 24, Dec. 2016, Art. no. 243901.

[10] J. Atulasimha, A. B. Flatau, and E. Summers, "Characterization and energy-based model of the magnetomechanical behavior of polycrystalline iron–gallium alloys," *Smart Mater. Struct.*, vol. 16, no. 4, pp. 1265–1276, Aug. 2007.

[11] A. Kumar and V. Sundararaghavan, "Simulation of magnetostrictive properties of galfenol under thermomechanical deformation," *Finite Elements Anal. Des.*, vol. 127, pp. 1–5, May 2017.

[12] M. Domenjoud, E. Berthelot, N. Galopin, R. Corcolle, Y. Bernard, and L. Daniel, "Characterization of giant magnetostrictive materials under static stress: Influence of loading boundary conditions," *Smart Mater. Struct.*, vol. 28, no. 9, Sep. 2019, Art. no. 095012.

[13] M. Domenjoud and L. Daniel, "Effects of plastic strain and reloading stress on the magneto-mechanical behavior of electrical steels: Experiments and modeling," *Mech. Mater.*, vol. 176, Jan. 2023, Art. no. 104510.

[14] L. Daniel and M. Domenjoud, "Anhysteretic magneto-elastic behaviour of Terfenol-D: Experiments, multiscale modelling and analytical formulas," *Materials*, vol. 14, no. 18, p. 5165, 2021.

[15] R. M. Bozorth, *Ferromagnetism*. New York, NY, USA: IEEE Press, 1951.

[16] O. Hubert and L. Daniel, "Measurement and analytical modeling of the ΔE effect in a bulk iron-cobalt alloy," *IEEE Trans. Magn.*, vol. 46, no. 2, pp. 401–404, Feb. 2010.

[17] L. Daniel and N. Galopin, "A constitutive law for magnetostrictive materials and its application to Terfenol-D single and polycrystals," *Eur. Phys. J. Appl. Phys.*, vol. 42, no. 2, pp. 153–159, May 2008.

[18] L. Bernard, B. J. Mailhé, N. Sadowski, N. J. Batistela, and L. Daniel, "Multiscale approaches for magneto-elasticity in device simulation," *J. Magn. Magn. Mater.*, vol. 487, Oct. 2019, Art. no. 165241.

[19] L. Daniel, M. Rekik, and O. Hubert, "A multiscale model for magneto-elastic behaviour including hysteresis effects," *Arch. Appl. Mech.*, vol. 84, nos. 9–11, pp. 1307–1323, Oct. 2014.

[20] L. Daniel, O. Hubert, N. Buiron, and R. Billardon, "Reversible magneto-elastic behavior: A multiscale approach," *J. Mech. Phys. Solids*, vol. 56, no. 3, pp. 1018–1042, Mar. 2008.

[21] A. Clark, M. Wun-Fogle, J. B. Restorff, and T. A. Lograsso, "Magnetostrictive properties of galfenol alloys under compressive stress," *Mater. Trans.*, vol. 43, no. 5, pp. 881–886, 2002.